Divalent and Trivalent α-Ketocarboxylic Acids as Inhibitors of Protein Tyrosine Phosphatases

Yen Ting Chen and Christopher T. Seto*

Department of Chemistry, Brown University, 324 Brook Street, Providence, Rhode Island 02912

Received February 28, 2002

Protein tyrosine phosphatases (PTPases) are important targets for the treatment of insulin resistance in patients with type II diabetes and as antibacterial agents. As a result, there is a growing interest in the development of potent and specific inhibitors for these enzymes. This paper describes a series of inhibitors that contain two or three α-ketocarboxylic acid groups that are designed to form multiple contacts with residues inside or near the active site of phosphatases. The inhibitors have been assayed against three PTPases: the *Yersinia* PTPase, PTP1B, and LAR. The best of the inhibitors has IC_{50} values against the *Yersinia* PTPase and PTP1B of 0.7 and 2.7 μM, respectively. These divalent and trivalent compounds are significantly more potent than their corresponding monovalent analogues. In addition, they show good selectivity for PTP1B and the *Yersinia* PTPase as compared to LAR.

Introduction

The coordinated activity of protein tyrosine phosphatases (PTPases) and kinases is critical for controlling the signal transduction pathways that regulate numerous cell functions. These functions include cell mitosis, growth factor responses, and insulin signaling.[1,2] PTPases were at first believed to be few in number and to serve merely as "housekeeping" enzymes.[3,4] However, recent studies have shown that PTPases encompass a large family of related enzymes, and several members have been linked to various forms of disease. For instance, the *Yersinia* and *Salmonella* bacteria both employ PTPases for their pathogenicity.[5,6] The *Yersinia* genus is comprised of three species that are responsible for diseases that include the bubonic plague and gastrointestinal syndromes.[7] Because bacteria are believed to contain no protein phosphotyrosines,[8] the targets of the *Yersinia* PTPase are most likely to be host proteins. In humans, overexpression of PTPases or elevation of PTPase activity is believed to contribute to type II diabetes and cancer.[9] PTP1B, the first PTPase to be isolated and characterized, has been implicated, along with several other PTPases such as LAR and PTPα, as negative regulators of the insulin receptor.[10] Knockout studies have demonstrated that mice lacking functional PTP1B show increased sensitivity to insulin and are resistant to diet-induced obesity, while still appearing to be normal and healthy.[11,12] Hence, development of specific, potent PTPase inhibitors is of significant interest because they may serve both as tools to study signal transduction pathways and as therapeutic agents.

A variety of PTPase inhibitors have been reported in the literature.[13] One approach for designing inhibitors is to replace a phosphotyrosine residue on a polypeptide substrate, such as the sequence derived from the epidermal growth factor receptor ($EGFR_{988-993}$, Ac-DADEpYL-NH_2), with a nonhydrolyzable pTyr mimic.[14,15] This method has led to the development of several potent inhibitors.[16,17] However, small molecule inhibitors are often more appealing due to the intrinsic problems with peptide-based therapeutics. Peptidic inhibitors are often subject to proteolytic degradation and show poor cell permeability, and these issues can be significant obstacles in the development of effective drugs.[15,18]

Because all members of the PTPase family possess the PTPase signature motif (H/V)**C**X_5**R**(S/T) in the catalytic domain,[19] generating selective inhibitors can be difficult. Zhang and co-workers have recently reported a noncatalytic, low-affinity aryl phosphate binding site that is adjacent to the active site in PTP1B.[20] This secondary site is defined by the key residues Arg-24, Arg-254, Met-258, Gly-259, and Gln-262. While residues such as Arg-254 and Gln-262 are invariant among PTPases,[21] some of the other residues of the secondary binding site are reported to be less conserved than the residues comprising the catalytic site. A crystal structure of the C215S mutant of PTP1B with bis-(*p*-phosphophenyl)methane (BPPM) (Chart 1) showed that BPPM binds in two modes. In one mode, one phosphate group of BPPM binds to the active site while the other forms a water-mediated hydrogen bond with Gln-262. In the second mode, one phosphate group forms a similar interaction with Gln-262, but the other phosphate occupies the secondary binding site. While one BPPM molecule cannot bind to both the catalytic and the secondary sites simultaneously, two separate pTyr molecules can bind to both sites simultaneously.[20]

Significant data in the literature indicate that substrates and inhibitors with two or more anionic groups display enhanced binding. The biphosphorylated insulin receptor kinase (IRK) activation peptide, ETDpYpYRKGGKGGL, exhibits a 70-fold greater affinity for PTP1B than its monophosphorylated analogue, ETDYpYRKGGKGGL, and has been shown to interact with Arg-24 and Arg-254 of the noncatalytic site.[22] Montserat and co-workers observed that BPPM exhibits a K_m of 16 μM. This value is 39 times lower than that of *p*-nitrophenyl

* To whom correspondence should be addressed. Tel: 401-863-3587. Fax: 401-863-2594. E-mail: Christopher_Seto@Brown.edu.

10.1021/jm020093q CCC: $22.00
Published on Web 07/12/2002

Chart 1. Structure of BPPM

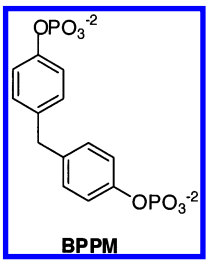

Chart 2. Structures of Compounds **1**−**6**

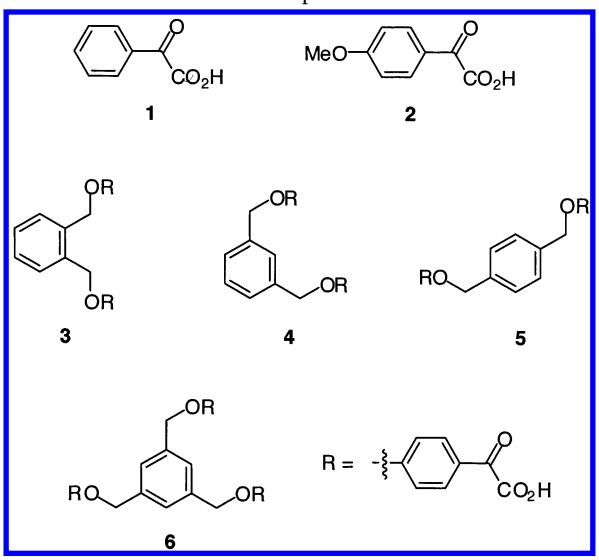

phosphate with rat PTP1 and is comparable to the best peptide substrates.[23] Ramachandran and co-workers found that tripeptides containing two difluoromethylphosphonophenylalanine (F_2Pmp) residues, such as E-F_2Pmp-F_2Pmp, are potent inhibitors of PTP1B with IC_{50} values in the nanomolar range. By comparison, the IC_{50} value of an analogous tripeptide with a single F_2-Pmp residue is 10 μM.[24] Recently, the Zhang and Taylor groups reported a number of inhibitors that bear two difluoromethylphosphonic acid (DFMP) units. These compounds are potent inhibitors of PTP1B with inhibition constants in the range of 0.93−12 μM.[25,26] Taken together, these observations all suggest that compounds possessing two appropriately spaced aryl phosphate mimics should show increased inhibitory potency and selectivity by binding to both the active site and the noncatalytic site.

We have previously reported that aryl α-ketocarboxylic acids can serve as the basis for PTPase inhibitors.[27] The aryl α-ketoacids are designed to make several contacts with residues in the PTPase catalytic site. These contacts include an electrostatic interaction between the carboxylate and the Arg of the signature motif, a hydrogen bond between the ketone oxygen and the Asp of the WPD loop, and hydrophobic interactions between the aryl ring and the nearby aromatic residues in the active site. We have also found that addition of an electron-donating group in the para position of the aryl ring results in increased potency. In particular, the *p*-methoxyphenylglyoxylic acid (**2**) (Chart 2) is a reasonable inhibitor of the *Yersinia* PTPase with an IC_{50} value of 150 μM. For comparison, benzoylformic acid (**1**) has a modest IC_{50} of 2.7 mM. This information, in conjunction with the dual-binder concept, has led us to design a series of divalent inhibitors that exhibit good selectivity and enhanced inhibition. In the present study, we report on the synthesis of compounds bearing two and three *p*-alkoxyphenylglyoxylic acid moieties (**3**−**6**) and evaluate their inhibitory properties against the *Yersinia* PTPase, PTP1B, and LAR.

Scheme 1[a]

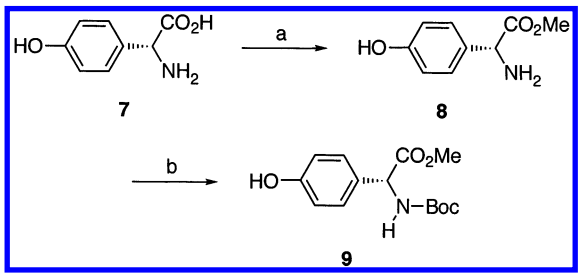

[a] Reagents: (a) $SOCl_2$, MeOH, 100%. (b) Boc_2O, $NaHCO_3$, 1:1 H_2O:dioxane, 95%.

Chart 3. Structures of Compounds **10**−**13**

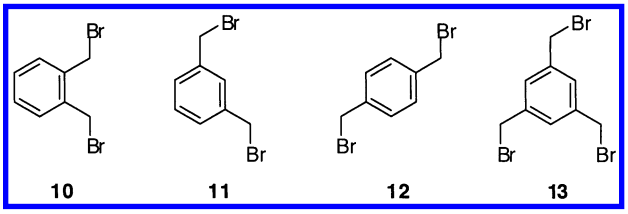

Chemistry

The syntheses of compounds **3**−**6** began with *D*-4-hydroxyphenylglycine **7** (Scheme 1). This is an inexpensive and readily available starting material that contains functional groups in all of the appropriate positions for incorporation into the final inhibitors. Our strategy was to convert the amino acid portion of **7** into the corresponding α-ketocarboxylic acid using a transamination reaction during a late stage of the syntheses.

Compound **7** was first converted to methyl ester **8** using thionyl chloride and methanol (Scheme 1). The amino group in **8** was then protected as the *tert*-butyl carbamate to give compound **9**. Williamson ether syntheses using compound **9** with di- and tribromides **10**−**13** (Chart 3) in the presence of sodium and ethanol yielded ethers **14**−**17** (Scheme 2). Tribromide **13** was prepared by treating mesitylene with *N*-bromosuccinimide and benzoyl peroxide according to the procedure of Vögtle.[28] During the Williamson ether syntheses, a transesterification reaction also occurred that converted the methyl esters into the corresponding ethyl esters. Removal of the Boc protecting groups in these compounds with trifluoroacetic acid gave amines **18**−**21** and set the stage for the transamination reaction.

Meldal and co-workers have recently reported a new method for synthesizing α-ketoamide-containing peptides on a solid support.[29] In this method, the free amino group at the N terminus of a peptide that is bound to a solid support is treated with glyoxylate and copper(II) sulfate at pH 5.5. Under these conditions, the copper(II) ion catalyzes a transamination reaction that converts the N-terminal amino acid into the corresponding α-ketoamide, while also converting glyoxylate into glycine. We have applied these reaction conditions to amino esters **18**−**21** in order to obtain the corresponding

Scheme 2[a]

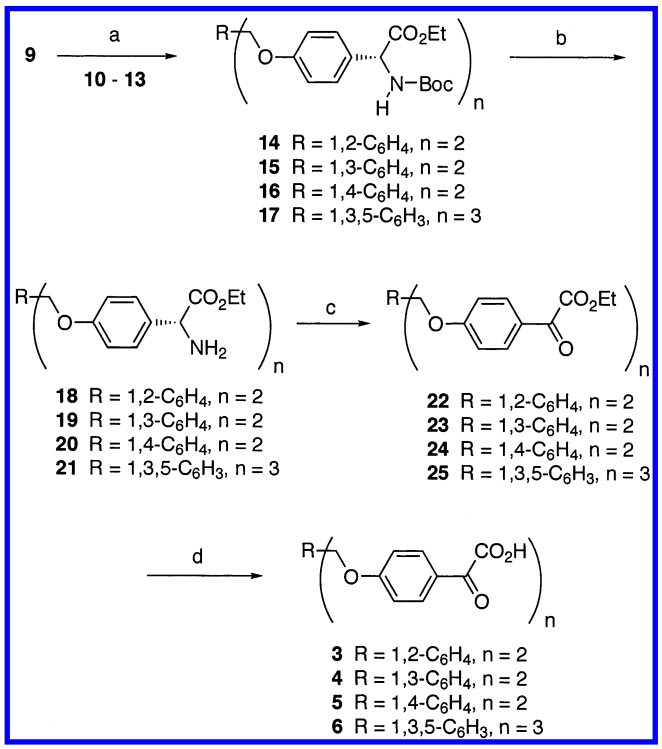

[a] Reagents: (a) Na, EtOH, **14** (43%), **15** (49%), **16** (47%), **17** (21%). (b) TFA, CH_2Cl_2, **18** (85%), **19** (91%), **20** (86%), **21** (89%). (c) HO_2CCHO, $CuSO_4$, AcOH, pyridine, **22** (16%), **23** (19%), **24** (21%), **25** (15%). (d) NaOH, H_2O, **3** (93%), **4** (69%), **5** (91%), **6** (57%).

Scheme 3[a]

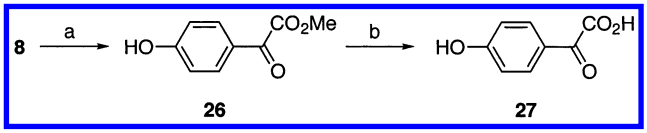

[a] Reagents: (a) HO_2CCHO, $CuSO_4$, AcOH, pyridine, 44%. (b) NaOH, H_2O, 82%.

α-ketoesters **22**−**25** (Scheme 2). The reactions proceeded in relatively low yield for these substrates that contain multiple amino ester groups, but a better yield was obtained for compound **8**, which contains only a single reactive amine (Scheme 3). Despite the modest yields, the product ketoesters were obtained reliably and in pure form by simple extraction followed by flash chromatography on silica gel. In previous work, we prepared a series of aryl α-ketocarboxylic acids by oxidation of arylmethyl ketones with selenium dioxide.[27] In comparing the two methods of synthesis, the selenium dioxide procedure gave higher yields, but the ketoacids were often contaminated with byproducts that were difficult to separate by chromatography. By contrast, the transamination procedure gave relatively clean products that were easy to purify. However, the yield was low for substrates that contained multiple amines.

The synthesis of inhibitors **3**−**6** was completed by hydrolysis of the esters with aqueous sodium hydroxide. The final α-ketoacid products precipitated from the hydrolysis reaction mixtures upon acidification with hydrochloric acid. The inhibitors were further purified using preparative reverse phase high-performance liquid chromatography (HPLC). For comparison with the di- and trifunctional inhibitors, we also prepared the monoketoacid **27** by transamination of methyl *D*-4-hydroxyphenylglycine **8** followed by hydrolysis of the methyl ester (Scheme 3).

Table 1. Inhibition of Phosphatases by α-Ketocarboxylic Acid-Based Inhibitors[a]

	IC_{50} (μM)		
compd	*Yersinia* PTPase	PTP1B	LAR
3	8.5 ± 0.8	19 ± 5	120 ± 30
4	4.1 ± 0.6	53 ± 8	120 ± 15
5	0.7 ± 0.2	2.7 ± 0.5	250 ± 70
6	1.7 ± 0.5	13 ± 3	41 ± 5
27	200 ± 20	250 ± 30	2300 ± 700

[a] Average of two measurements.

Results and Discussion

Inhibitors **3**−**6** and **27** were assayed against three PTPases: the *Yersinia* PTPase, PTP1B, and LAR. The *Yersinia* PTPase, an essential virulence determinant for the pathogenic bacterium,[30] is an intracellular enzyme with a structure that is similar to PTP1B.[31,32] This phosphatase is believed to possess the residues that make up the secondary binding site. LAR is a transmembrane receptor-like phosphatase that, along with PTP1B, plays a role in regulating insulin receptor signaling.[33−36] LAR was included in our study because it is a different type of PTPase from *Yersinia* or PTP1B and lacks the residues that correspond to the noncatalytic secondary binding site. All assays were performed using *p*-nitrophenyl phosphate as the substrate at 25 °C with 100 mM NaCl and 100 mM acetate buffer at pH 5.5. The results are summarized in Table 1.

The monomeric compound **27** is a poor inhibitor of LAR and a modest inhibitor of the *Yersinia* PTPase and PTP1B. The potency of **27** against the *Yersinia* PTPase is slightly weaker than compound **2**, the methoxy counterpart (IC_{50} = 150 μM).[27] By contrast, the multivalent compounds are significantly better inhibitors of the *Yersinia* PTPase than **27** or any of the other monomeric α-ketoacids that we have studied to date.

Compounds with two *p*-alkoxyphenylglyoxylic acid moieties (**3**−**5**) exhibit inhibitory potencies up to 280 times greater than **27** against the *Yersinia* PTPase and up to 90 times greater against PTP1B. These compounds are modest inhibitors of LAR, with IC_{50} values between 120 and 250 μM. Of these compounds, compound **5** stands out as the most potent inhibitor of the *Yersinia* PTPase and PTP1B, having IC_{50} values of 0.7 and 2.7 μM against the two enzymes, respectively. In addition, compound **5** is 90-fold more selective for PTP1B than for LAR. These values are comparable to the bis-DFMP inhibitors that have been reported recently by other groups, where the IC_{50} values against PTP1B are in the range of 0.9−12 μM and selectivity for PTP1B over LAR ranges from 5- to 130-fold.[25,26] We have found that the variation in IC_{50} values among **3**−**5** is a factor of 10−20, with compound **5**, the 1,4-disubstituted system, being the most potent. These results can be contrasted with the results of Jia and co-workers using divalent DFMP inhibitors that contain a similar phenyl ether linkage (**28**−**30**) (Chart 4).[26] In their report, the differences among **28**−**30** were a factor of 3, with the 1,2-system (**28**) being the most potent.

Chart 4. Structures of Compounds **28**−**30**

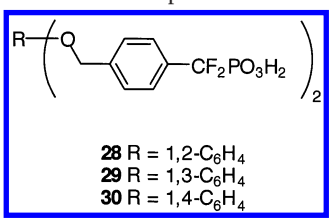

Chart 5. Structures of Compounds **31** and **32**

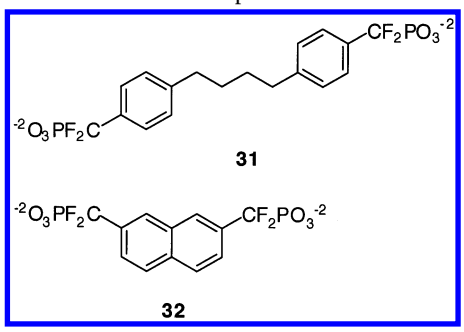

We have also prepared the tridentate inhibitor **6**. The IC_{50} values for compound **6** against the *Yersinia* PTPase and PTP1B (1.7 and 13 μM, respectively) fall within the range set by the other bidentate compounds. It is the most potent LAR inhibitor of the series (IC_{50} = 41 μM), although its activity against LAR is significantly lower than its activity against the other two PTPases. Compound **6** still shows selectivity for the *Yersinia* PTPase and PTP1B over LAR by 24- and 3-fold, respectively. Taken together, our results show that *p*-alkoxyaryl α-ketoacids can serve as the basis for designing potent phosphatase inhibitors. Because α-ketoacids are monoanionic, they may show enhanced cell permeability when compared to phosphonic acids and other dianionic phosphotyrosine mimics.[37]

What is the binding mode of these bidentate ligands? Taing et al. reported an extensive series of PTPase inhibitors with two DFMP groups that exhibit preference for PTP1B over VHR, LAR, and PTPα.[25] The observed selectivity could be attributed to simultaneous binding to both the catalytic and the secondary sites. It is also possible that the second DFMP interacts with positively charged residues outside of the noncatalytic site. Jia and co-workers studied the crystal structures of PTP1B complexed with inhibitors **31** and **32** (Chart 5).[26] In both complexes, one of the DFMP groups bound to the active site while the other was extended into the solvent to form a water-mediated hydrogen bond with Arg-47. In two other examples, the guanidium side chain of Arg-47 was found to form a hydrogen bond with an Asp residue on the IRK activation loop[22] and with the Glu residue on the Ac-DADE-X-L-NH_2 peptide that has been used as a platform for peptide-based inhibitors.[38] It is not clear if other bidentate inhibitors, such as compounds **3**−**5**, follow the same mode of binding. Divalent inhibitors that bind in the catalytic site and the secondary binding site may have similar inhibition constants as those that bind in the active site and with Arg-47.

Preliminary molecular modeling studies using the published X-ray structure of PTP1B[20] were performed to rationalize the binding mode of compounds **3**−**5**. Of these inhibitors, compounds **4** and **5** appear to be capable of binding to both the active site and Arg-47. Compound **3** does not appear to be long enough for one α-ketoacid moiety to bind to Arg-47 while the other is anchored in the catalytic site by residues such as Arg-221. Instead, it appears more favorable for **3** to interact with some of the residues that constitute the secondary site, such as Gln-262. By comparison, compounds **4** and **5** are able to interact with the active site and either Arg-47 or to the secondary binding site.

Conclusions

We have synthesized a series of inhibitors that are based on the α-ketocarboxylic acid motif. These compounds are potent inhibitors of the *Yersinia* PTPase and PTP1B and show good selectivity for these phosphatases as compared to LAR. The bidentate and tridentate inhibitors are all more potent than compounds with only one α-ketoacid, and they have IC_{50} values that are comparable to structurally similar DFMP-based inhibitors. We have not yet established the mode of binding of these multivalent inhibitors. The results presented in this work, along with other inhibitors that have been reported previously in the literature, show that tethering two PTPase inhibiting moieties together with an appropriate linker is an effective strategy for enhancing the selectivity and potency of phosphatase inhibitors.

Experimental Section

General Methods. Nuclear magnetic resonance (NMR) spectra were recorded on Bruker Avance-300 or Avance-400 instruments. Spectra were calibrated using tetramethylsilane (TMS) (δ = 0.00 ppm) for ^{1}H NMR and $CDCl_3$ (δ = 77.0 ppm) or dimethyl sulfoxide (DMSO) (δ = 39.5 ppm) for ^{13}C NMR. Mass spectra were recorded on either a Kratos MS 80 under electron impact (EI), chemical ionization (CI), or fast atom bombardment (FAB) conditions or on an Applied Biosystems QSTAR electrospray mass spectrometer. HPLC analyses were performed on a Rainin HPLC system with Rainin Microsorb silica or C18 columns and UV detection. Semipreparative HPLC was performed on the same system using a semipreparative column (21.4 mm × 250 mm).

Reactions were conducted under an atmosphere of dry nitrogen in oven-dried glassware. Solvents were of reagent grade and were stored over 4 Å molecular sieves. All reagents were used as received. Solvent removal was performed by rotary evaporation at water aspirator pressure.

***D*-4-Hydroxyphenylglycine Methyl Ester (8).** *D*-4-Hydroxyphenylglycine (**7**, 10.0 g, 60.1 mmol) was suspended in methanol (200 mL), and thionyl chloride (8 mL) was added dropwise. After the resulting mixture was stirred at room temperature for 10 h, the solvent was removed by rotary evaporation and the residue was washed twice with ether to yield *D*-4-hydroxyphenylglycine methyl ester as a white solid (13.0 g, 60.0 mmol, 100%). ^{1}H NMR (300 MHz, DMSO-d_6): δ 3.68 (s, 3 H), 5.07 (s, 1 H), 6.85 (d, J = 8.5 Hz, 2 H), 7.29 (d, J = 8.6 Hz, 2 H), 9.03 (s, 3 H), 10.02 (s, 1 H). ^{13}C NMR (75 MHz, DMSO-d_6): δ 53.8, 55.8, 116.5, 123.4, 130.5, 159.4, 170.0. HRMS-FAB (M + H^+) calcd for $C_9H_{12}NO_3$, 182.0817; found, 182.0811.

***N*-Boc-*D*-4-hydroxyphenylglycine Methyl Ester (9).** To a mixture **8** (2.60 g, 12.0 mmol) and $NaHCO_3$ (1.51 g, 18.0 mmol) in H_2O (25 mL) was added Boc anhydride (3.13 g, 14.3 mmol) in dioxane (25 mL). The mixture was stirred for 1 h at 0 °C and then 6 h at room temperature. After it was acidified with 1 N HCl to approximately pH 2, the mixture was extracted with three portions of ethyl acetate (50 mL). The organic layer was combined and washed with H_2O (100 mL) and brine (100 mL) and dried over Na_2SO_4, and the solvent was removed by rotary evaporation to yield *N*-Boc-*D*-4-hydroxyphenylglycine methyl ester as a white solid (3.18 g, 11.3 mmol,

95%). ^{1}H NMR (300 MHz, $CDCl_3$): δ 1.45 (s, 9 H), 3.71 (s, 3 H), 5.23 (d, J = 7.1 Hz, 1 H), 5.61 (d, J = 6.5 Hz, 1 H), 6.56 (s, 1 H), 6.75 (d, J = 8.6 Hz, 2 H), 7.17 (d, J = 8.1 Hz, 2 H). ^{13}C NMR (75 MHz, $CDCl_3$): δ 28.7, 53.1, 57.5, 80.9, 116.2, 128.6, 128.8, 147.2, 155.5, 172.4. HRMS-FAB (M + Na^+) calcd for $C_{14}H_{19}NNaO_5$, 304.1161; found, 304.1166.

Representative Procedure for the Synthesis of Compounds 14−17. Compound 15. To a solution of sodium (0.302 g, 13.1 mmol) dissolved in ethanol (50 mL) was added **9** (3.09 g, 11.0 mmol) and then α,α′-dibromo-*m*-xylene (**11**, 1.61 g, 4.40 mmol). The mixture was stirred continuously at room temperature for 23 h under a N_2 atmosphere, the solvent was removed, and the residue was treated with H_2O (30 mL) and ethyl acetate (30 mL). The layers were separated, and the aqueous layer was extracted with two portions of ethyl acetate (30 mL). The organic layers were combined and washed with H_2O (30 mL), twice with a saturated solution of aqueous Na_2CO_3 (30 mL), and brine (30 mL), dried over Na_2SO_4, and concentrated to dryness. Purification by flash column chromatography (1:1 hexane:ethyl ether) yielded compound **15** (1.49 g, 2.15 mmol, 49%) as white foam. ^{1}H NMR (300 MHz, $CDCl_3$): δ 1.23 (t, J = 7.1 Hz, 6 H), 1.45 (s, 18 H), 4.19 (m, 4 H), 5.08 (s, 4 H), 5.25 (d, J = 7.3 Hz, 2 H), 5.53 (d, J = 6.6 Hz, 2 H), 6.96 (d, J = 8.7 Hz, 4 H), 7.30 (d, J = 8.7 Hz, 4 H), 7.41 (s, 3 H), 7.50 (s, 1 H). ^{13}C NMR (75 MHz, $CDCl_3$): δ 14.4, 28.7, 57.5, 62.1, 70.2, 80.5, 115.5, 126.9, 127.5, 128.8, 129.3, 129.9, 137.6, 155.3, 159.1, 171.8. ESI (M + H^+) calcd for $C_{38}H_{49}N_2O_{10}$, 693.3387; found, 693.3369.

Compound 14. Yield, 43%. ^{1}H NMR (300 MHz, $CDCl_3$): δ 1.23 (t, J = 7.1 Hz, 6 H), 1.45 (s, 18 H), 4.19 (m, 4 H), 5.16 (s, 4 H), 5.25 (d, J = 7.9 Hz, 2 H), 5.52 (m, 2 H), 6.95 (d, J = 8.4 Hz, 4 H), 7.29 (d, J = 8.4 Hz, 4 H), 7.39 (dd, J = 5.6, 3.3 Hz, 2 H), 7.52 (dd, J = 5.5, 3.5 Hz, 2 H). ^{13}C NMR (75 MHz, $CDCl_3$): δ 14.4, 28.7, 57.4, 62.1, 68.4, 80.4, 115.5, 128.8, 129.0, 129.4, 130.1, 135.3, 155.2, 159.0, 171.7. ESI (M + H^+) calcd for $C_{38}H_{49}N_2O_{10}$, 693.3387; found, 693.3407.

Compound 16. Yield, 47%. ^{1}H NMR (300 MHz, $CDCl_3$): δ 1.23 (t, J = 7.1 Hz, 6 H), 1.45 (s, 18 H), 4.19 (m, 4 H), 5.07 (s, 4 H), 5.25 (d, J = 6.9 Hz, 2 H), 5.51 (d, J = 6.6 Hz), 6.96 (d, J = 8.7 Hz, 4 H), 7.30 (d, J = 8.7 Hz, 4 H), 7.45 (s, 4 H). ^{13}C NMR (75 MHz, $CDCl_3$): δ 14.4, 28.7, 57.5, 62.1, 70.1, 80.4, 115.5, 128.1, 128.8, 130.0, 137.1, 155.2, 159.1, 171.7. ESI (M + H^+) calcd for $C_{38}H_{49}N_2O_{10}$, 693.3387; found, 693.3395.

Compound 17. Yield, 21%. ^{1}H NMR (300 MHz, $CDCl_3$): δ 1.23 (t, J = 7.1 Hz, 9 H), 1.45 (s, 27 H), 4.20 (m, 6 H), 5.09 (s, 6 H), 5.26 (d, J = 7.1 Hz, 3 H), 5.54 (d, J = 6.0 Hz, 3 H), 6.96 (d, J = 8.7 Hz, 6 H), 7.31 (d, J = 8.7 Hz, 6 H) 7.46 (s, 3 H). ^{13}C NMR (75 MHz, $CDCl_3$): δ 14.4, 28.7, 57.5, 62.1, 70.1, 80.5, 115.5, 126.4, 128.8, 130.1, 138.2, 155.2, 159.1, 171.7. ESI (M + H^+) calcd for $C_{54}H_{70}N_3O_{15}$, 1000.4807; found, 1000.4817.

Representative Procedure for the Synthesis of Compounds 18−21. Compound 19. Compound **15** (1.85 g, 2.67 mmol) was dissolved in a solution of 20% trifluoroacetic acid (TFA) in methylene chloride (10 mL), and the solution was stirred in an ice bath for 2 h. The solvent was removed, and the residue was taken up in methylene chloride (30 mL) and washed twice with a saturated solution of aqueous $NaHCO_3$ (20 mL). The organic layer was dried over Na_2SO_4, and the solvent was removed by rotary evaporation to yield compound **19** (1.19 g, 2.42 mmol, 91%) as a clear oil. ^{1}H NMR (300 MHz, DMSO-d_6): δ 1.11 (t, J = 7.1 Hz, 6 H), 2.19 (s, 4 H), 4.04 (m, 4 H), 4.42 (s, 2 H), 5.09 (s, 4 H), 6.96 (d, J = 8.5 Hz, 4 H), 7.28 (d, J = 8.5 Hz, 4 H), 7.39 (s, 3 H), 7.51 (s, 1 H). ^{13}C NMR (75 MHz, DMSO-d_6): δ 14.9, 55.8, 58.4, 61.1, 69.9, 115.4, 127.7, 128.0, 129.4, 134.3, 138.2, 158.5, 175.1. ESI (M + H^+) calcd for $C_{28}H_{33}N_2O_6$, 493.2339; found, 493.2344.

Compound 18. Yield, 85%. ^{1}H NMR (300 MHz, DMSO-d_6): δ 1.12 (t, J = 7.1 Hz, 6 H), 2.21 (s, 4 H), 4.04 (s, 4 H), 4.42 (s, 2 H), 5.21 (s, 4 H), 6.97 (d, J = 8.7 Hz, 4 H), 7.28 (d, J = 8.7 Hz, 4 H), 7.36 (dd, J = 5.6, 3.4 Hz, 2 H), 7.51 (dd, J = 5.4, 3.4 Hz, 2 H). ^{13}C NMR (75 MHz, DMSO-d_6): δ 14.9, 58.5, 61.1, 112.7, 115.4, 128.8, 129.3, 134.4, 136.0, 158.4, 175.0. ESI (M + H^+) calcd for $C_{28}H_{33}N_2O_6$, 493.2339; found, 493.2340.

Compound 20. Yield, 86%. ^{1}H NMR (300 MHz, DMSO-d_6): δ 1.12 (t, J = 7.1 Hz, 6 H), 2.21 (s, 4 H), 4.04 (m, 4 H), 4.42 (s, 2 H), 5.09 (s, 4 H), 6.95 (d, J = 8.7 Hz, 4 H), 7.28 (d, J = 8.7 Hz, 4 H), 7.44 (s, 4 H). ^{13}C NMR (75 MHz, DMSO-d_6): δ 14.9, 58.4, 61.1, 69.8, 115.4, 128.6, 128.8, 134.2, 137.6, 158.4, 175.0. ESI (M + H^+) calcd for $C_{28}H_{33}N_2O_6$, 493.2339; found, 493.2327.

Compound 21. Yield, 89%. ^{1}H NMR (300 MHz, DMSO-d_6): δ 1.12 (t, J = 7.1 Hz, 9 H), 2.17 (s, 6 H), 4.05 (m, 6 H), 4.43 (s, 3 H), 5.12 (s, 6 H), 6.97 (d, J = 7.6 Hz, 6 H), 7.29 (d, J = 7.8 Hz, 6 H), 7.48 (s, 3 H). ^{13}C NMR (75 MHz, DMSO-d_6): δ 14.9, 58.4, 61.1, 69.8, 115.4, 127.2, 128.8, 134.3, 138.5, 158.4, 175.1. ESI (M + H^+) calcd for $C_{39}H_{46}N_3O_9$, 700.3234; found, 700.3252.

Representative Procedure for the Synthesis of Compounds 22−25. Compound 23. To a solution of **19** (0.344 g, 0.70 mmol) in dioxane (6 mL) was added a freshly prepared aqueous solution (10 mL) of glyoxylic acid (0.736 g, 8.0 mmol) and copper(II) sulfate pentahydrate (200 mg, 0.80 mmol) in a buffer containing 2.5 M pyridine and 0.5 M acetic acid. The mixture was stirred overnight at room temperature and then extracted with three portions of methylene chloride (25 mL). The organic layers were combined, washed twice with 1 N HCl (20 mL), dried over Na_2SO_4, and then concentrated to dryness. The residue was purified by flash column chromatography ($CHCl_3$) to yield **23** (66.4 mg, 0.14 mmol, 19%) as clear oil. ^{1}H NMR (300 MHz, $CDCl_3$): δ 1.44 (t, J = 7.1 Hz, 6 H), 4.45 (q, J = 7.1 Hz, 4 H), 5.20 (s, 4 H), 7.07 (d, J = 8.9 Hz, 4 H), 7.44 (m, 3 H), 7.52 (s, 1 H), 8.04 (d, J = 8.9 Hz, 4 H). ^{13}C NMR (75 MHz, $CDCl_3$): δ 14.5, 62.6, 70.4, 115.4, 126.3, 126.8, 127.8, 129.6, 133.0, 136.9, 164.3, 164.5, 185.2. ESI (M + H^+) calcd for $C_{28}H_{27}O_8$, 491.1706; found, 491.1721.

Compound 22. Yield, 16%. ^{1}H NMR (300 MHz, DMSO-d_6): δ 1.31 (t, J = 7.1 Hz, 6 H), 4.39 (q, J = 7.1 Hz, 4 H), 5.39 (s, 4 H), 7.21 (d, J = 8.9 Hz, 4 H), 7.42 (dd, J = 5.5, 3.5 Hz, 2 H), 7.56 (dd, J = 5.5, 3.5 Hz, 2 H), 7.91 (d, J = 8.9 Hz, 4 H). ^{13}C NMR (75 MHz, DMSO-d_6): δ 14.7, 63.0, 68.6, 116.4, 125.6, 129.4, 129.8, 133.1, 135.3, 164.7, 165.0, 186.1. ESI (M + Na^+) calcd for $C_{28}H_{26}NaO_8$, 513.1526; found, 513.1502.

Compound 24. Yield, 21%. ^{1}H NMR (300 MHz, $CDCl_3$): δ 1.44 (t, J = 7.1 Hz, 6 H), 4.45 (q, J = 7.1 Hz, 4 H), 5.19 (s, 4 H), 7.06 (d, J = 8.8 Hz, 4 H), 7.48 (s, 4 H), 8.03 (d, J = 8.8 Hz, 4 H). ^{13}C NMR (75 MHz, $CDCl_3$): δ 14.5, 62.6, 70.3, 115.4, 126.2, 128.3, 133.0, 136.4, 164.4, 164.5, 185.2. ESI (M + Na^+) calcd for $C_{28}H_{26}NaO_8$, 513.1526; found, 513.1514.

Compound 25. Yield, 15%. ^{1}H NMR (300 MHz, $CDCl_3$): δ 1.44 (t, J = 7.1 Hz, 9 H), 4.45 (q, J = 7.1 Hz, 6 H), 5.21 (s, 6 H), 7.07 (d, J = 8.9 Hz, 6 H), 7.50 (s, 3 H), 8.04 (d, J = 8.9 Hz, 6 H). ^{13}C NMR (75 MHz, $CDCl_3$): δ 14.5, 62.6, 70.1, 115.4, 126.4, 126.6, 133.1, 137.6, 164.2, 164.4, 185.1. ESI (M + H^+) calcd for $C_{39}H_{37}O_{12}$, 697.2285; found, 697.2306.

Representative Procedure for the Synthesis of Compounds 3−6. Compound 4. To a solution of compound **23** (66.4 mg, 0.135 mmol) in methanol (2 mL) was added 2.5 M NaOH (2 mL). The mixture was stirred at 50 °C for 1 h, cooled, and acidified with concentrated HCl to approximately pH 2. The precipitate was collected by centrifugation and then resuspended in water (5 mL). Addition of ethyl acetate (5 mL) dissolved the precipitate, and after the layers were separated, the aqueous layer was extracted twice with ethyl acetate (5 mL). The ethyl acetate layers were combined, dried over Na_2SO_4, and concentrated to dryness to yield **4** as a yellow solid (40.5 mg, 0.093 mmol, 69%). The compounds were purified further by HPLC (see the Supporting Information). ^{1}H NMR (300 MHz, DMSO-d_6): δ 5.27 (s, 4 H), 7.22 (d, J = 8.8 Hz, 4 H), 7.46 (s, 3 H), 7.59 (s, 1 H), 7.89 (d, J = 8.8 Hz, 4 H). ^{13}C NMR (75 MHz, DMSO-d_6): δ 70.4, 116.3, 125.8, 128.2, 128.5, 129.7, 132.8, 137.4, 164.5, 167.4, 188.1. ESI (M − H^+, negative ion mode) calcd for $C_{24}H_{17}O_8$, 433.0923; found, 433.0932.

Compound 3. Yield, 93%. ^{1}H NMR (300 MHz, DMSO-d_6): δ 5.38 (s, 4 H), 7.22 (d, J = 8.9 Hz, 4 H), 7.41 (dd, J = 5.5, 3.5 Hz, 2 H), 7.56 (dd, J = 5.5, 3.5 Hz, 2 H), 7.89 (d, J = 8.9 Hz, 4 H). ^{13}C NMR (75 MHz, DMSO-d_6): δ 68.5, 116.3, 125.8,

129.4, 129.8, 132.8, 135.4, 164.4, 167.3, 188.0. ESI ($M - H^+$, negative ion mode) calcd for $C_{24}H_{17}O_8$, 433.0923; found, 433.0921.

Compound 5. Yield, 91%. ^{1}H NMR (300 MHz, DMSO-d_6): δ 5.26 (s, 4 H), 7.22 (d, $J = 8.8$ Hz, 4 H), 7.50 (s, 4 H), 7.90 (d, $J = 8.8$ Hz, 4 H). ^{13}C NMR (75 MHz, DMSO-d_6): δ 70.3, 115.5, 116.3, 125.7, 128.9, 132.9, 137.0, 164.5, 167.3, 188.0. ESI ($M - H^+$, negative ion mode) calcd for $C_{24}H_{17}O_8$, 433.0923; found, 433.0938.

Compound 6. Yield, 57%. ^{1}H NMR (300 MHz, DMSO-d_6): δ 5.30 (s, 6 H), 7.22 (d, $J = 8.9$ Hz, 6 H), 7.58 (s, 3 H), 7.90 (d, $J = 8.8$ Hz, 6 H). ^{13}C NMR (75 MHz, DMSO-d_6): δ 70.3, 116.3, 125.8, 127.9, 132.8, 137.8, 164.4, 167.4, 188.1. ESI ($M - H^+$, negative ion mode) calcd for $C_{33}H_{23}O_{12}$, 611.1190; found, 611.1214.

Methyl 4-Hydroxyphenylglyoxylate (26). Compound **8** (0.302 g, 1.39 mmol) was dissolved in a freshly prepared aqueous solution of glyoxylic acid (1.27 g, 13.8 mmol) and copper(II) sulfate pentahydrate (0.35 g, 1.40 mmol) in a buffer containing 2.5 M pyridine and 0.5 M acetic acid. The mixture was stirred for 10 h at room temperature and then extracted with three portions of methylene chloride (10 mL). The organic layers were combined, washed three times with 0.5 M HCl (20 mL), dried over Na_2SO_4, and concentrated to dryness. Purification by flash column chromatography ($CHCl_3$) yielded methyl 4-hydroxyphenylglyoxylate as a clear oil (0.109 g, 6.06 mmol, 44%). ^{1}H NMR (300 MHz, $CDCl_3$): δ 3.99 (s, 3 H), 5.41 (br s, 1 H), 6.95 (d, $J = 8.8$ Hz, 2 H), 8.00 (d, $J = 8.8$ Hz, 2 H). ^{13}C NMR (75 MHz, $CDCl_3$): δ 53.1, 116.3, 126.2, 133.4, 161.9, 164.7, 184.8. ESI ($M - H^+$, negative ion mode) calcd for $C_9H_8O_4$, 179.0344; found, 179.0341.

4-Hydroxyphenylglyoxylic Acid (27). Compound **26** (52.1 mg, 0.289 mmol) was dissolved in 2.5 M NaOH (2 mL), and the mixture was stirred for 2 h at room temperature. After it was washed twice with diethyl ether (5 mL), the aqueous layer was acidified with concentrated HCl to approximately pH 2 and extracted with three portions of ethyl acetate (5 mL). The combined ethyl acetate extracts were washed with brine (10 mL), dried over Na_2SO_4, and concentrated to dryness to yield **27** as a yellow solid (39.4 mg, 0.237 mmol, 82%). ^{1}H NMR (300 MHz, DMSO-d_6): δ 6.94 (d, $J = 8.8$ Hz, 2 H), 7.81 (d, $J = 8.8$ Hz, 2 H), 10.82 (br s, 1 H). ^{13}C NMR (75 MHz, DMSO-d_6): δ 116.9, 124.1, 133.2, 164.7, 167.6, 187.8. ESI ($M - H^+$, negative ion mode) calcd for $C_8H_6O_4$, 165.0188; found, 165.0186.

***Yersinia* PTPase and LAR Assays.** The phosphatase activities of the *Yersinia* PTPase and LAR (purchased from Calbiochem) were assayed using *p*-NPP as the substrate, and the reaction progress was monitored by UV spectroscopy. Initial rates were determined by monitoring the hydrolysis of *p*-NPP at 420 nm, from 10 to 120 s after mixing. Assay solutions contained 2.5 mM substrate, 1 mM EDTA, 100 mM NaCl, 100 mM acetate at pH 5.5, and 10% DMSO. IC_{50} values were calculated using a Dixon analysis. Data analysis was performed with the commercial graphing package Grafit (Erithacus Software Ltd.). The K_m values under these conditions were found to be 2.5 and 2.1 mM for the *Yersinia* PTPase and LAR, respectively.

PTP1B Assay. PTP1B (purchased from Calbiochem) was assayed using *p*-NPP as the substrate, and the reaction progress was monitored by UV spectroscopy. Initial rates were determined by monitoring the hydrolysis of *p*-NPP at 420 nm, from 10 to 120 s after mixing. Assay solutions contained 1.2 mM substrate, 1 mM EDTA, 100 mM NaCl, 100 mM acetate at pH 5.5, and 10% DMSO. IC_{50} values were calculated using a Dixon analysis. Data analysis was performed with the commercial graphing package Grafit (Erithacus Software Ltd.). The K_m value under these conditions was measured to be 0.62 mM. The K_m value in the absence of DMSO and in acetate buffer at pH 5.5 is reported to be 0.75 mM.[39]

Molecular Modeling. Molecular modeling studies were performed using CHARMm (version 23.2) running on Silicon Graphics Indy 4400 workstation. The X-ray structure of PTP1B bound to BPPM (PDB entry 1AAX) was used as the starting structure for the modeling work. Compounds **3**−**5** were constructed using QUANTA and then docked into the catalytic site using the BPPM ligand that was present in the original structure as a basis for initial placement. This system was minimized with 2000 iterations using an Adjusted Basis Newton−Raphson algorithm as implemented in the CHARMm program.

Acknowledgment. This research was supported by the NIH (Grant GM57327).

Supporting Information Available: HPLC characterization for compounds **3**−**6** and **27**. This material is available free of charge via the Internet at http://pubs.acs.org.

References

(1) Hunter, T. Protein kinases and phosphatases: the yin and yang of protein phosphorylation and signaling. *Cell* **1995**, *80*, 225−236.
(2) Fauman, E.; Saper, M. A. Structure and function of the protein tyrosine phosphatase. *Trends Biochem. Sci.* **1996**, *21*, 413−417.
(3) Neel, B. G.; Tonks, N. K. Protein tyrosine phosphatase in signal transduction. *Curr. Opin. Cell. Biol.* **1997**, *9*, 193−204.
(4) Zhang, Z.-Y. Protein tyrosine phosphatases: prospects for therapeutics. *Curr. Opin. Cell. Biol.* **2001**, *5*, 416−423.
(5) Bliska, J. B.; Guan, K. L.; Dixon, J. E.; Falkow, S. Tyrosine phosphate hydrolysis of host proteins by an essential *Yersinia* virulence determinant. *Proc. Natl. Acad. Sci. U.S.A.* **1991**, *88*, 1187−1891.
(6) Kaniga, K.; Uralil, J.; Bliska, J. B.; Galan, J. E. A secreted protein tyrosine phosphatase with modular effector domains in the bacterial pathogen *Salmonella typhimurium*. *Mol. Microbiol.* **1996**, *21*, 633−641.
(7) Butler, T. *Plague and other Yersinia infections*; Plenum Press: New York, 1983; pp 31−64.
(8) Foster, R.; Thorner, J.; Martin, G. S. Nucleotidylation, not phosphorylation, is the major source of the phosphotyrosine detected in enteric bacteria. *J. Bacteriol.* **1989**, *171*, 272−279.
(9) Hunter, T. Signaling−2000 and beyond. *Cell* **2000**, *100*, 113−127.
(10) Goldstein, B. J.; Li, P.-M.; Ding, W.; Ahmad, F.; Zhang, W.-R. Regulation of insulin action by protein tyrosine phosphatases. *Vitam. Horm.* **1998**, *54*, 67−96.
(11) Elchebly, M.; Payette, P.; Michaliszyn, E.; Cromlish, W.; Collins, S.; Loy, A. L.; Normandin, D.; Cheng, A.; Himms-Hagen, J.; Chan, C.-C.; Ramachandran, C.; Gresser, M. J.; Tremblay, M. L.; Kennedy, B. P. Increased insulin sensitivity and obesity resistance in mice lacking the protein tyrosine phosphatase-1B gene. *Science* **1999**, *283*, 1544−1548.
(12) Klaman, L. D.; Boss, O.; Peroni, O.; Peroni, O. D.; Kim, J. K.; Martino, J. L.; Zablotny, J. M.; Moghal, N.; Lubkin, M.; Kim, Y.-B.; Sharpe, A. H.; Stricker-Krongrad, A.; Shulman, G. I.; Neel, B. G.; Kahn, B. B. Increased energy expenditure, decreased adiposity, and tissue-specific insulin sensitivity in protein-tyrosine phosphatase 1B-deficient mice. *Mol. Cell. Biol.* **2000**, *20*, 5479−5489.
(13) Ripka, W. C. Protein tyrosine phosphatase inhibition. *Ann. Rep. Med. Chem.* **2000**, *35*, 231−250.
(14) Gao, Y.; Wu, L.; Luo, J. H.; Guo, R.; Yang, D.; Zhang, Z.-Y.; Burke, T. R., Jr. Examination of novel non-phosphorus-containing phosphotyrosyl mimetics against protein-tyrosine phosphatase-1B and demonstration of differential affinities toward Grb2 SH2 Domains. *Bioorg. Med. Chem. Lett.* **2000**, *10*, 923−927.
(15) Burke, T. R., Jr.; Zhang, Z.-Y. Protein-tyrosine phosphatases: structure, mechanism, and inhibitor discovery. *Biopolymers* **1998**, *47*, 225−241.
(16) Burke, T. R., Jr.; Kole, H. K.; Roller, P. P. Potent inhibition of insulin receptor dephosphorylation by a hexamer peptide containing the phosphotyrosyl mimetic F_2Pmp. *Biochem. Biophys. Res. Commun.* **1994**, *204*, 129−134.
(17) Burke, T. R., Jr.; Bin, Y.; Akamatsu, M.; Ford, H., Jr.; Yan, X.; Kole, H. K.; Wolf, G.; Shoelson, S. E.; Roller, P. P. 4′-*O*-[2-(2-Fluoromalonyl)]-L-tyrosine: a phosphotyrosyl mimic for the preparation of signal transduction inhibitory peptides. *J. Med. Chem.* **1996**, *39*, 1021−1027.
(18) Taylor, S. D.; Kotoris, C. C.; Dinaut, N.; Wang, Q.; Ramachandran, C.; Huang, Z. Potent nonpeptidyl inhibitors of protein tyrosine phosphate 1B. *Bioorg. Med. Chem.* **1998**, *6*, 1457−1568.
(19) Zhang, Z.-Y.; Wang, Y.; Wu, L.; Stuckey, J. A.; Schubert, H. L.; Saper, M. A.; Dixon, J. E. The $Cys(X)_5Arg$ catalytic motif in phosphoester hydrolysis. *Biochemistry* **1994**, *33*, 15266−15270.
(20) Puius, Y. A.; Zhao, Y.; Sullivan, M.; Lawrence, D. S.; Almo, S. C.; Zhang, Z.-Y. Identification of a second aryl phosphate-binding site in protein tyrosine phosphatase 1B: a paradigm for inhibitor design. *Proc. Natl. Acad. Sci. U.S.A.* **1997**, *94*, 13420−13425.

(21) Zhang, Z. Y.; Wang, Y.; Dixon, J. E. Dissecting the catalytic mechanism of protein-tyrosine phosphatases. *Proc. Natl. Acad. Sci. U.S.A.* **1994**, *91*, 1624−1627.
(22) Salmeen, A.; Andersen, J. N.; Myers, M. D.; Tonks, N. K.; Barford, D. Molecular basis for dephosphorylation of the activation segment of the insulin receptor by protein tyrosine phosphate 1B. *Mol. Cell.* **2000**, *6*, 1401−1412.
(23) Montserat, J.; Chen, L.; Lawrence, D. S.; Zhang, Z.-Y. Potent low molecular weight substrates for protein-tyrosine phosphatase. *J. Biol. Chem.* **1996**, *271*, 7868−7872.
(24) Desmarais, S.; Friesen, R. W.; Zamboni, R.; Ramachandran, C. [Difluoro(phosphono)methyl]phenylalanine-containing peptide inhibitors of protein tyrosine phosphatases. *Biochem. J.* **1999**, *337*, 219−223.
(25) Taing, M.; Keng, Y.-F.; Shen, K.; Wu, L.; Lawrence, D. S.; Zhang, Z.-Y. Potent and highly selective inhibitors of the protein tyrosine phosphatase 1B. *Biochemistry* **1999**, *38*, 3793−3803.
(26) Jia, Z.; Ye, Q.; Dinaut, A. N.; Wang, Q.; Waddleton, D.; Payette, P.; Ramachandran, C.; Kennedy, B.; Hum, G.; Taylor, S. D. Structure of protein tyrosine phosphatase 1B in complex with inhibitors bearing two phosphotyrosine mimics. *J. Med. Chem.* **2001**, *44*, 4584−4594.
(27) Chen, Y. T.; Onaran, M. B.; Doss, C. J.; Seto, C. T. α-Ketocarboxylic acid-based inhibitors of protein tyrosine phosphatases. *Bioorg. Med. Chem. Lett.* **2001**, *11*, 1935−1938.
(28) Vögtle, F.; Zuber, M.; Lichtenthaler, R. G. Notiz über ein vereinfachtes verfahren zur darstellung von 1,3,5-tris(bromomethyl)benzol. *Chem. Ber.* **1973**, *106*, 717−718.
(29) Papanikos, A.; Rademann, J.; Meldal, M. α-Ketocarbonyl Peptides: A general approach to reactive resin-bound intermediates in the synthesis of peptide isosteres for protease inhibitor screening on solid support. *J. Am. Chem. Soc.* **2001**, *123*, 2176−2181.
(30) Guan, K. L.; Dixon, J. E. Protein tyrosine phosphatase activity of an essential virulence determinant in *Yersinia*. *Science* **1990**, *249*, 553−555.
(31) Barford, D.; Flint, A. J.; Tonks, N. K. Crystal structure of human protein tyrosine phosphatase 1B. *Science* **1994**, *263*, 1397−1404.
(32) Stuckey, J. E.; Schubert, H. L.; Fauman, E. B.; Zhang, Z.-Y.; Dixon, J. E.; Saper, M. A. Crystal structure of *Yersinia* protein tyrosine phosphatase at 2.5 Å and the complex with tungstate. *Nature* **1994**, *370*, 571−575.
(33) Mooney, R. A.; Kulas, D. T.; Bleyle, L. A.; Novak, J. S. The protein tyrosine phosphatase LAR has a major impact on insulin receptor dephosphorylation. *Biochem. Biophys. Res. Commun.* **1997**, *235*, 709−712.
(34) Ahmad, F.; Goldstein, B. J. Functional association between the insulin receptor and the transmembrane protein-tyrosine phosphatase in intact cells. *J. Biol. Chem.* **1997**, *272*, 448−457.
(35) Tsai, A. Y. M.; Itoh, M.; Streuli, M.; Thai, T.; Saito, H. Isolation and characterization of temperature-sensitive and thermostable mutants of the human receptor-like protein tyrosine phosphatase LAR. *J. Biol. Chem.* **1991**, *266*, 10534−10543.
(36) Zabolotny, J. M.; Kim, Y.-B.; Perone, J. K.; Pani, M. A.; Boss, O.; Klamar, L. D.; Kamatkar, S.; Shulman, G. I.; Kahn, B. B.; Neel, B. G. Overexpression of the LAR (leukocyte antigen-related) protein-tyrosine phosphatase in muscle causes insulin resistance. *Proc. Natl. Acad. Sci. U.S.A.* **2001**, *98*, 5187−5192.
(37) Kole, H. K.; Smyth, M. S.; Russ, P. L.; Burke, T. R., Jr. Phosphatase inhibitors of protein-tyrosine and serine/threonine phosphatases. *Biochem. J.* **1995**, *311*, 1025−1031.
(38) Jia, Z.; Barford, D.; Flint, A. J.; Tonks, N. K. Structural basis for phosphotyrosine peptide recognition by protein tyrosine phosphatase 1B. *Science* **1995**, *268*, 1754−1758.
(39) Iversen, L. F.; Andersen, H. S.; Branner, S.; Mortensen, S. B.; Peters, G. H.; Norris, K.; Olsen, O. H.; Jeppesen, C. B.; Lundt, B. F.; Ripka, W.; Moller, K. B.; Moller, N. P. H. Structure-based design of a low molecular weight, nonphosphorus, nonpeptide, and highly selective inhibitor of protein-tyrosine phosphatase 1B. *J. Biol. Chem.* **2000**, *275*, 10300−10307.

JM020093Q